Optimal Quasi-Orthogonal FH Sequences with Adaptive Array Receiver for Massive Connectivity in Asynchronous Multi-Cluster Networks

Qi Zeng, *Member, IEEE,* Zilong Liu, *Senior Member, IEEE,* and Gradoni Gabriele, *Member, IEEE*

***Abstract*—This paper is concerned with the enabling of massive connectivity in a multi-cluster network. In order to tackle significant amount of interference imposed by inter- and intra-cluster users, we consider a frequency-hopping (FH) system where an improved quasi-orthogonal hopping pattern, called optimal strong no-hit-zone FH sequence (SNHZ-FHS) set, is adopted in each cluster. We propose a flexible construction of SNHZ-FHS sets and derive their Hamming correlation values at different access delays. Since the maximum number of supportable users under traditional FH networks is strictly limited by the number of frequency slots, we investigate the design of a novel class of adaptive array beam-forming (BF) receiver in which SNHZ-FHS patterns (i.e., SNHZ-FH/BF) are reused over asynchronous multi-cluster uplink channels. Extensive numerical comparisons show that our proposed SNHZ-FH/BF system provides an effective means for attaining higher user capacity as well as remarkable capability of interference suppression.**

***Index Terms*—Optimal FH, beamforming receiver, sequence design, interference suppression, performance analysis, multi-cluster networks**

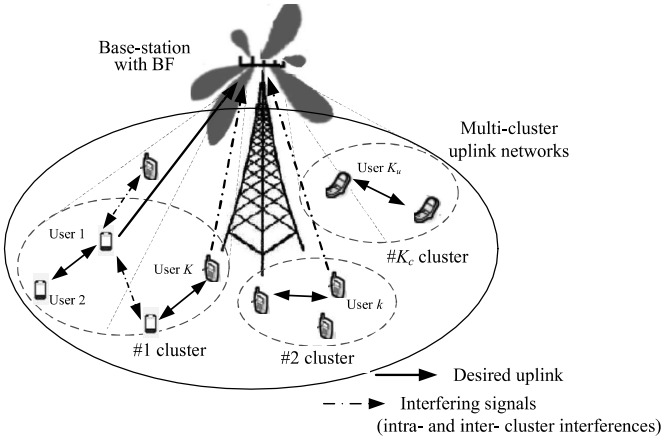

Fig. 1. An illustration of multi-cluster uplink communications, where the desired link (labelled by the solid black line) is impaired by interfering inter- and intra-cluster signals.

I. Introduction

A. Background

The unprecedented evolution of wireless communication systems has led to an explosive growth of mobile devices which are widely present in a diverse range of wireless networks, such as 5G/B5G cellular networks, vehicle-to-everything communications, sensor networking, etc. Each of these networks may be comprised of multi-clusters in which limited communication resources (e.g., space, time, code, and spectrum) are shared among all users [1, 2]. As shown in Fig. 1, a massive number of users is partitioned into multiple disjoint user-clusters according to their locations and quality-of-service (QoS) requirements, where the communication of the desired uplink (labelled by the solid black line) may be impaired by interfering intra- and inter-cluster signals. On the other hand, the spectrum (in particular, the sub-6 GHz spectrum band) is becoming increasingly congested, resulting in ever-growing interference and potentially jamming attacks in wireless networks. To support massive connectivity, it is pressing to investigate effective approaches for improved interference suppression/mitigation.

Q. Zeng is with the College of Electrical Engineering, Sichuan University, Chengdu 610065, China. This work was supported in part by National Science Foundation of China under Grant 61701328 and in part by Foundation of Science and Technology on Communication Security Laboratory of China under Grant No. 6142103200106. (Corresponding author: Q. Zeng. E-mail: qzeng1@hotmail.com).

Z. Liu is with the School of Computer Science and Electronics Engineering, University of Essex, Colchester CO4 3SQ, U.K. (e-mail: zilong.liu@essex.ac.uk).

G. Gabriele is with the School of Mathematical Science and also with the Department of Electrical and Electronic Engineering, University of Nottingham, Nottingham NG7 2RD, U.K. (e-mail: gabriele.gradoni@nottingham.ac.uk).

B. Objective and Motivations

This paper aims to design an enhanced frequency-hopping (FH) communication system which is capable of supporting larger user capacity as well as superior anti-interference performances in asynchronous multi-cluster networks. Over the past decades, FH communications have received tremendous research attention owing to their strong resilience to interference/jamming and thus significantly enhanced robustness in various harsh communication environments [3–5]. The FH sequences (also called FH patterns) are one of the most important components to determine the entire system performance. In the past engineering practice, certain pseudo-random FH patterns, with which the frequency-hits follow a near uniform-distribution over arbitrary access delays, are studied in [6–10]. With the ever-growing communication devices, the traditional pseudo-random FH patterns and reception approaches may yield tremendously compromised FH system performance (e.g., in terms of user capacity, error rate probability). For asynchronous multi-cluster FH communication networks, it is desirable to develop new FH sequence sets and novel receiver

design approaches which can serve a massive number of users, whilst maintaining (almost) orthogonality properties using a minimum number of frequency-slots.

In the literature, there have been some design criteria of pseudo-random FH patterns that are subject to several Hamming correlation (i.e., the number of frequency-hits) lower bounds, e.g., Lempel bound and Peng-Fan bound [6, 11]. A pseudo-random FH pattern may be said to be *optimal* if it meets one of the Hamming correlation lower bounds [12–14]. For mitigation of multi-access interference (MAI), orthogonal FH sequence sets are desired for frequency hit-free performances. Driven by this objective, recently, a quasi-orthogonal hopping pattern, called no-hit-zone FH sequence (NHZ-FHS) set, has attracted increasing research attention. As its name conveys, an NHZ-FHS set owns the orthogonality for small access delays around the origin [15–17, 19]. In [18], we have proposed an improved quasi-orthogonal FH pattern, called strong NHZ-FH sequence (SNHZ-FHS) set, which enjoys orthogonality (i.e., frequency hit-free) for certain small access delays as well as minimum frequency-hits otherwise. A new Hamming correlation lower bound of SNHZ-FHS set has also been derived in [18]. Such an *optimal* SNHZ-FHS set is promising for the mitigation/suppression of interference in a single cluster with asynchronous access delays. A similar idea has been adopted in quasi-synchronous direct-sequence spread spectrum (DSSS) systems using zero-correlation-zone sequences [20, 21].

In this paper, we are concerned with future multi-cluster networks, in which interference may arise within certain intra-cluster and from multiple inter-clusters. It is noted that 1) the maximum number of supportable users of the existing FHS sets (including traditional pseudo-random FH pattern, NHZ-FHS, SNHZ-FHS and so forth) is strictly constrained by the number of frequency slots [11, 18], and 2) reusing FH pattern alone in multi-cluster may not be able to attain a good performance due to the potentially huge amount of interference.

C. Contributions

Our first contribution is a new systematic construction of *optimal* SNHZ-FHS sets. Our derivation of the Hamming correlation values shows that, given a minimum frequency-slots, the developed SNHZ-FHS set enjoys the least frequency-hits with guaranteed orthogonality (i.e., frequency-hits free) for certain small access delays[1]. In comparison with [18] where an SNHZ-FHS set is generated by multiple seed FH sets with specific Hamming correlation properties, our proposed construction is implemented by selecting only one pseudo-random FHS set as the seed set, thus greatly simplifying the construction procedure.

Aiming towards massive connectivity in future wireless systems with limited spectrum, we then propose an adaptive beam-forming (BF) receiver for SNHZ-FH based multi-cluster networks, where the resultant system is called SNHZ-FH/BF. As shown in Fig. 1, we propose the idea of designing an adaptive array receiver at the base-station (BS) to generate the main-lobe to cover the area of the desired user-cluster, and null-lobes to cover interferers [22–24], helping to remove a large portion of inter-cluster interference. Within each desired cluster, the intra-cluster interference is mitigated/suppressed by assigning our developed SNHZ-FH patterns to the active users. The detailed receiver structure is depicted in Fig. 2 which will be discussed in detail in Section IV.

As a case study, we employ a direct-matrix-inversion (DMI) BF algorithm based on the least-mean-square criterion (LMS) to adaptively adjust the beam-pattern. Compared to other adaptive algorithms in [24], the LMS-DMI algorithm can rapidly generate a stable beam-pattern with the aid of a short-length pilot signal. Moreover, we carry out theoretical analysis for the bit-error-rate (BER) performance of the proposed SNHZ-FH/BF system. Our derived BER is shown to be a function of various SNHZ-FH parameters and BF parameters, shedding some light on the impact of these factors in terms of their individual anti-interference capabilities. Our extensive numerical comparisons demonstrate that the proposed SNHZ-FH/BF system is capable of accommodating massive number of users, whilst enjoying significantly reduced interference and hence excellent BER performances.

It should be pointed out that our proposed SNHZ-FH/BF system is different to the previous studies which integrate BF with traditional FH patterns only [25–27]. These previous works may not attain good BER performances due to large frequency-hits resulting from interfering users and an in-depth theoretical analysis of their anti-interference capabilities is missing. Compared with many existing transmission technologies, our proposed SNHZ-FH/BF system exhibits the following advantages for its application in multi-cluster networks:

- Compared with the DS-SS technique, FH is more flexible as it can adaptively choose the blank spectral bands to avoid the risk of interference causing from the licensed and the unlicensed bands. Also, FH is relatively easy to integrate into the existing wireless applications[2].
- Compared with traditional pseudo-random FH (e.g., [12–14]), our proposed SNHZ-FH/BF system can provide both the (quasi-)orthogonality and high spectral efficiency with no need of strict synchronization.
- In contrast to our earlier proposed SNHZ-FH system [18] with a single antenna and targeting single-cluster networks only[3], the unique interference mitigation capabilities of our proposed SNHZ-FH/BF system stem from the adopted BF technique for adaptively selecting a desired cluster (thus, helping to avoid the interference from neighboring clusters) and the designed optimal SNHZ-FHS set for supporting active users therein. Thus, our proposed SNHZ-FH/BF system provides a promising means for the support of multi-cluster networks with the massive number of users in future wireless systems.

[1]Note that frequency-hits may not be avoided for some known pseudo-random FH patterns [7–10, 12–14].

[2]An excellent introduction on application of FH in narrowband IoT can be found in [28].

[3]Throughput this paper, such an SNHZ-FH system is also called a traditional SNHZ-FH system.

D. Organization of This Paper

The remainder of this paper is organized as follows. Section II presents a brief introduction and the basic properties of several optimal FH patterns, e.g., (strong) NHZ-FHS and traditional pseudo-random FHS. This is followed by a new construction of the optimal SNHZ-FHS set as well as the derivation of its Hamming correlation values in Section III. In Section IV, we apply the proposed optimal SNHZ-FHS set to an adaptive BF receiver for asynchronous multi-cluster uplink networks. As a case study, in Section V, we consider the proposed SNHZ-FH/BF system using the M-ary frequency-shift keying modulation (FSK) and the adaptive LMS-DMI algorithm, and analyze its anti-interference capability from the viewpoints of the spectral and spatial dimensions. In Section VI, we derive the theoretical BER performance of the proposed system as a function of the SNHZ-FH and BF parameters. We validate these theoretical results through MATLAB simulations in Section VII. Finally, this paper is concluded in Section VIII. A list of acronyms and variables of this paper is given in Table I.

TABLE I
LIST OF ACRONYMS AND VARIABLES

Acronyms	Descriptions
5G/B5G	The 5th generation and beyond
BER	Bit-error-rate
BF	Beamforming
DMI	Direct-matrix-inversion
DoA	Direction of arrival
FH	Frequency-hopping
ISI	Inter-symbol interference
LMS	Least-mean-square criterion
MAI	Multiple-access interference
MFSK	M-ary frequency-shift keying modulation
NHZ	No-hit-zone
SNHZ	Strong no-hit-zone
SINR	Signal-to-interference-plus-noise ratio
ULA	Uniform linear array
Variables	**Descriptions**
$\mathbf{a}_n^{(i)}$	Array steering-vector for the i-th cluster
$\mathbb{C}$	Proposed SNHZ-FH sequence set
$d_n^{(i,k)}$	Transmitted symbol of the k-th user in the i-th cluster at the n-th interval
$h(x,y)$	Frequency hit or hit-free function
H_a	Maximum Hamming auto-correlation
H_c	Maximum Hamming cross-correlation
H_m	Maximum Hamming correlation
$I^{(i,k)}(t)$	MAI resulting from the k-th user in the i-th cluster
$I_{\text{inter}}(t)$	Inter-cluster interference
$I_{\text{intra}}(t)$	Intra-cluster interference
K	Size of FH sequence set
K_c	Number of clusters
K_u	Total number of users in networks
L	Length of FH sequence
N_a	Number of array elements
P_k	Transmitted signal power of the k-th user
q	Size of frequency slot set
$\mathbb{S}$	Traditional FH sequence set
$\tau^{(i,k)}$	Access delay of the k-th user in the i-th cluster
T	Interval of an MFSK symbol (a hopping slot interval)
U_l	Decision variable of demodulator
$\mathbf{w}_{DMI}$	Optimal weights of array elements
Z	Width of no-hit zone

II. PRELIMINARIES

In this section, we present the individual definitions of several optimal FHS sets (i.e., NHZ-FHS, SNHZ-FHS and traditional pseudo-random FHS) and then recall their Hamming correlation lower bounds.

A. NHZ-FH Pattern

***Definition* 1.** *[16]: Let $\mathbb{S} = \{S^{(k)}, k = 1, 2, \cdots, K\}$ denote a sequence set with size K, where $S^{(k)} = \left(s^{(k)}(0), s^{(k)}(1), s^{(k)}(2), \cdots, s^{(k)}(L-1)\right), s^{(k)}(i) \in GF(q)$ is an FH sequence for the k-th user with length L and size of frequency-slots q. The FH sequence set $\mathbb{S}$ is called an NHZ-FHS with no-hit zone Z, when its Hamming auto-correlation ($H_{uu}(\tau)$) and Hamming cross-correlation ($H_{uv}(\tau)$) satisfy the following conditions, respectively:*

$$\begin{aligned} Z_a &= \max_{0<|\tau|\le T_d}\{T_d | H_{uu}(\tau) = 0, \forall S^{(u)} \in \mathbb{S}\}, \\ Z_c &= \max_{0\le|\tau|\le T_d}\{T_d | H_{uv}(\tau) = 0, \forall S^{(u)}, S^{(v)} \in \mathbb{S}, u \ne v\}, \\ Z &= \min\{Z_a, Z_c\}, \end{aligned} \tag{1}$$

where T_d stands for the possible range of shift-delay. The periodic Hamming correlation function under the integer shift τ is denoted as

$$H_{uv}(\tau) = \sum\nolimits_{i=0}^{L-1} h\left(s^{(u)}(i), s^{(v)}(i+\tau)\right) . \tag{2}$$

The index addition $(i+\tau)$ in the above equation is performed with respect to modulo L. If $x = y$, then $h(x,y) = 1$; otherwise $h(x,y) = 0$. By convention, an NHZ-FHS set is denoted by $\mathbb{S}(q, L, K, Z)$. ■

The fundamental tradeoffs of the four parameters q, L, K, Z of an NHZ-FHS are characterized by the Ye-Fan bound below.

***Theorem* 1.** *Ye-Fan bound [16, 19]:*

$$\left\lfloor \frac{L}{Z+1} \right\rfloor \ge \frac{KL}{q}, \tag{3}$$

where $\lfloor y \rfloor$ denotes the largest integer not greater than y. An NHZ-FHS set is said to be optimal *when the above inequality is met with equality. The Ye-Fan bound has been widely used for the design of optimal NHZ-FHS sets [15–17].*

From ***Definition 1***, it is observed that the Hamming auto- and cross-correlations of an optimal NHZ-FHS set are equal to zero (i.e., orthogonality) for small shift-delays satisfying $|\tau| \le Z$. On the other hand, when $|\tau| > Z$, a large amount of frequency hits for long shift-delays may be present, implying potential performance deterioration imposed by inter-symbol interference (ISI) and MAI in asynchronous FH communication networks.

B. SNHZ-FH Pattern

Next, we respectively define the maximum Hamming auto- and cross-correlations of the above NHZ-FHS set $\mathbb{S}$ for the case of $|\tau| > Z$ as follows:

$$\begin{aligned} H_a &= \max\left\{H_{uu}(\tau) | S^{(u)} \in \mathbb{S}, Z+1 \le |\tau| \le L-1\right\}, \\ H_c &= \max\left\{H_{uv}(\tau) | S^{(u)}, S^{(v)} \in \mathbb{S}, u \ne v, Z+1 \le |\tau| \le L-1\right\}. \end{aligned}$$

The maximum Hamming correlation for $|\tau| > Z$ is defined as

$$H_m = \max\{H_a, H_c\}. \tag{4}$$

A fundamental tradeoff among q, L, K, Z, H_m has been established in [18] as follows.

***Lemma* 1.** *Hamming correlation lower bound of SNHZ-FHS set:*

$$H_m \geq \frac{KL^2 - qL}{q\left\lfloor \frac{L}{Z+1} - 1 \right\rfloor + q(K-1)\left\lfloor \frac{L}{Z+1} \right\rfloor}. \tag{5}$$

***Definition* 2.** *[18]: An NHZ-FHS set achieving the equality in both (3) and (5) is called an* optimal *SNHZ-FHS set, which is denoted by $\mathbb{S}(q, L, K, Z, H_m)$ for simplicity.*

From ***Definition 2*** and for a given frequency-slot set with size q, we have the following remarks for an *optimal* SNHZ-FHS set $\mathbb{S}(q, L, K, Z, H_m)$:

- The maximum Hamming correlation enjoys orthogonality for small access delays $|\tau| \leq Z$ (i.e., quasi-synchronous access), whilst having minimum amount of frequency-hits for $|\tau| > Z$, as indicated by H_m in (5).
- In this case, all other parameters, i.e., the length of FHS L, the size of FHS set K, the width of orthogonal zone Z, approach to the maximum.
- However, the size of an optimal SNHZ-FHS set K is subject to the size of the frequency-slots set q, which implies that SNHZ-FH alone is unable to support the massive user connectivity. This motivates us to propose the SNHZ-FH/BF based receiver in Section IV.

C. Traditional Peng-Fan FH Pattern

Given an FHS set $\mathbb{S} = \{S^{(k)}, k = 1, 2, \cdots, K\}$ with the parameters (q, L, K), we define the maximum Hamming auto- and cross-correlations of $\mathbb{S}$ when the delay is extended over the entire sequence period L as follows, respectively.

$$H_a = \max\left\{H_{uu}(\tau)|S^{(u)} \in \mathbb{S}, 0 < |\tau| \leq L-1\right\},$$
$$H_c = \max\left\{H_{uv}(\tau)|S^{(u)}, S^{(v)} \in \mathbb{S}, u \neq v, |\tau| \leq L-1\right\}.$$

Then, a *Peng-Fan* FHS set is defined as follows.

***Definition* 3.** *[11]: An FHS set $\mathbb{S}$ with the parameters (q, L, K, H_m), where $H_m = \max\{H_a, H_c\}$, is called an* optimal Peng-Fan FHS set*, when the Hamming correlation lower bound on H_m below (i.e., the Peng-Fan bound) is met with equality:*

$$H_m \geq \left\lceil \frac{(LK-q)L}{(LK-1)q} \right\rceil. \tag{6}$$

Traditional Peng-Fan FHS set is a widely known class of FH patterns for FHMA systems but may suffer from certain nonzero Hamming correlations over arbitrary access delays. Systematic constructions of Peng-Fan FHS sets have been proposed in [10–14]. In this paper, a Peng-Fan FHS set is referred to as a traditional *optimal pseudo-random* FHS set.

III. Proposed Construction of Optimal SNHZ-FHS Set and its Hamming Correlation Properties

In this section, we introduce a new construction of *optimal* SNHZ-FHS set which enjoys simpler synthesis procedure than that in [18]. Then we present and prove the Hamming correlation values of the proposed SNHZ-FHS, followed by a step-by-step example.

A. New Construction of Optimal SNHZ-FHS Set and Its Properties

Step 1: We choose an optimal Peng-Fan FHS set $\mathbb{S} = \{S^{(1)}, S^{(2)}, \cdots, S^{(K_s)}\}$ as a seed set (denoted by $\mathbb{S}(q_s, L_s, K_s, H_s)$), where the Hamming cross-correlation at zero shift-delay $H_{uv}(0|\mathbb{S}) = 0$. The k-th sequence in $\mathbb{S}$ is written as

$$S^{(k)} = \left(s^{(k)}(0), s^{(k)}(1), \cdots, s^{(k)}(L_s-1)\right) \quad k = 1, 2, \cdots, K_s, \tag{7}$$

where $s^{(k)}(l) \in GF(q_s)$ for all k's and l's. This seed sequence set $\mathbb{S}$ can be readily obtained from the previous studies as shown in [12–14].

Step 2: Given a positive integer Z, we construct an optimal SNHZ-FHS set $\mathbb{C} = \{C^{(1)}, C^{(2)}, \cdots, C^{(K)}\}$ with size K and the k-th FHS $C^{(k)} = \left(c^{(k)}(0), c^{(k)}(1), \cdots, c^{(k)}(L-1)\right)$, where

$$c^{(k)}(m) = s^{(k)}(a) + bq_s, \quad \bmod q_s(Z+1), \quad m = 0, 1, \cdots, L-1; k = 1, 2, \cdots, K, \tag{8}$$

where $a = \lfloor \frac{m}{Z+1} \rfloor$, $b = m \mod (Z+1)$ and L denotes the length of sequence in $\mathbb{C}$.

***Theorem* 2.** *The above constructed $\mathbb{C} = \{C^{(1)}, C^{(2)}, \cdots, C^{(K)}\}$ is an SNHZ-FHS set with the NHZ width of Z, the number of sequences $K = K_s$ and the length of sequence $L = L_s(Z+1)$, over a given frequency-slot set with size $q = q_s(Z+1)$. The individual Hamming auto- and cross-correlation values are shown as*

$$H_{uu}(\tau) = \begin{cases} L, & \tau = 0, \\ H_{uu}(\tau|\mathbb{S})(Z+1), & \tau = l(Z+1), l \in \mathbb{N}^+, \\ 0, & \text{otherwise} \end{cases} \tag{9}$$

$$H_{uv}(\tau) = \begin{cases} H_{uv}(\tau|\mathbb{S})(Z+1), & \tau = l(Z+1), l \in \mathbb{N}^+ \\ 0, & \text{otherwise} \end{cases}, \quad u \neq v. \tag{10}$$

From Eqs. (9)-(10), the maximum Hamming correlation of $\mathbb{C}$ is obtained as $H_m = \max\{H_{uu}(\tau), H_{uv}(\tau)\} = (Z+1)H_s$. Moreover, the obtained set $\mathbb{C}$ is optimal *with respect to both the Ye-Fan bound in (3) and the SNHZ-FHS bound in (5).*

Proof. Since the length of the seed sequence set $\mathbb{S}$ is equal to L_s, we obtain $a = \lfloor \frac{m}{Z+1} \rfloor \leq L_s$ and $m \leq L_s(Z+1)$, according to **Step 2**. This implies that the length of the proposed FH set $L = L_s(Z+1)$.

From **Step 1**, the seed sequence set $\mathbb{S}$ is generated over the frequency slots set with size q_s. Since $b = m \mod (Z+1)$

in **Step 2**, we have $0 \le b \le Z$. Thus, according to (8), the total number of frequency slots in $\mathbb{C}$ is equal to $q_s(Z+1)$.

Next, we prove the Hamming cross-correlation value of (10). Given any two distinct sequences $C^{(u)}$ and $C^{(v)}, u \neq v$ of the proposed sequence set $\mathbb{C}$, let us assume that there exists at least one hit when their shift-delay $\tau \neq l(Z+1), l \in \mathbb{N}^+$, i.e.,

$$c^{(u)}(m_1) = c^{(v)}(m_2), \quad m_1 - m_2 = \tau. \tag{11}$$

According to (8) of the proposed construction, it is noted that the indices m_1, m_2 can be rewritten as $m_1 = a_1(Z+1)+b_1$ and $m_2 = a_2(Z+1)+b_2$, where a_1 (or a_2) and b_1 (or b_2) are analogy to a and b as shown in (8), respectively. Then, based on (11), we have

$$\begin{aligned} &c^{(u)}(m_1) - c^{(v)}(m_2) \\ &\qquad = s^{(v)}(a_1) - s^{(v)}(a_2) + (b_1 - b_2)q_s = 0. \end{aligned} \tag{12}$$

Since the seed sequence set $\mathbb{S}$ is generated from $GF(q_s)$ as shown in (7), one can easily have

$$s^{(u)}(a_1) - s^{(v)}(a_2) \in \{-q_s+1, -q_s+2 \cdots, q_s-2, q_s-1\}. \tag{13}$$

Besides, since b_1 or $b_2 \in \{0, 1, \cdots, Z-1, Z\}$, we have

$$(b_1 - b_2)q_s \in \{-Zq_s, (-Z+1)q_s, \cdots, (Z-1)q_s, Zq_s\}. \tag{14}$$

Thus, observed from (13) and (14), in order to make (12) equal to zero, the following equation should be satisfied:

$$s^{(u)}(a_1) = s^{(v)}(a_2), \quad \text{and} \quad b_1 = b_2. \tag{15}$$

From (15), it can be deduced that

$$m_1 = a_1(Z+1) + b_1 \text{ and } m_2 = a_2(Z+1) + b_2, \tag{16}$$

namely,

$$m_1 - m_2 = (a_1 - a_2)(Z+1) = l(Z+1). \tag{17}$$

This equation violates the assumption above. Thus, there is no hit between any two distinct sequences when $\tau \neq l(Z+1), l \in \mathbb{N}^+$, i.e., the Hamming cross-correlation $H_{u,v}(\tau) = 0$ for $\tau \neq l(Z+1), l \in \mathbb{N}^+$.

Otherwise, when $\tau = l(Z+1), l \in \mathbb{N}^+$, we have

$$c^{(v)}(m+\tau) = s^{(v)}\,(a+l) + bq_s. \tag{18}$$

Then the Hamming cross-correlation $H_{u,v}(\tau)$ is shown to be

$$\begin{aligned} H_{uv}(\tau) &= \sum_{m=0}^{L-1} h\left(c^{(u)}(m), c^{(v)}(m+\tau)\right) \\ &= \sum_{a=0}^{L_s-1} \sum_{b=0}^{Z} h\left(s^{(u)}(a) + bq_s, s^{(v)}\,(a+l) + bq_s\right) \\ &= (Z+1) \sum_{a=0}^{L_s-1} h\left(s^{(u)}(a), s^{(v)}(a+l)\right) \\ &= (Z+1)H_{uv}(\tau|\mathbb{S}), \quad \tau = l(Z+1), l \in \mathbb{N}^+. \end{aligned} \tag{19}$$

Since the maximum Hamming correlation of the seed sequence set $\mathbb{S}$ is assumed to be H_s as shown in **Step 1**, the Hamming cross-correlation of $\mathbb{C}$ for the case of $\tau = l(Z+1), l \in \mathbb{N}^+$ can be written as

$$H_{uv}(\tau) \le (Z+1)H_s. \tag{20}$$

Hence, this completes the proof of (10). The proof of (9) is similar to that of (10) by setting $u = v$, which is omitted to save space of this paper.

Based on the above parameters of the proposed sequence set $\mathbb{C}(q, L, K, Z, H_m) = \mathbb{C}(q_s(Z+1), L_s(Z+1), K_s, Z, H_s(Z+1))$, it is easy to validate that $\mathbb{C}$ meets with equality with respect to the bounds (3) and (5).

This completes the proof of ***Theorem 2***. □

B. An Example of the Proposed SNHZ-FHS Set

Following the proposed construction, an example of optimal SNHZ-FHS set is presented in this subsection. We choose a seed sequence set $\mathbb{S}$ which is generated over $GF(5)$ as follows.

$$\begin{aligned} \mathbb{S} = \{&(0,2,3,2,0); (2,1,4,1,2); (1,3,0,3,1); \\ &(3,4,2,4,3); (4,0,1,0,4)\}. \end{aligned}$$

It is easy to check that the maximum Hamming correlation of $\mathbb{S}(q_s, L_s, K_s, H_s) = (5,5,5,1)$ meets the Peng-Fan bound with equality. Given an integer $Z = 2$, an optimal SNHZ-FHS set can be obtained as follows according to (8).

$$\begin{aligned} \mathbb{C} = \{ \quad &(0,5,10,2,7,12,3,8,13,2,7,12,0,5,10); \\ &(2,7,12,1,6,11,4,9,14,1,6,11,2,7,12); \\ &(1,6,11,3,8,13,0,5,10,3,8,13,1,6,11); \\ &(3,8,13,4,9,14,2,7,12,4,9,14,3,8,13); \\ &(4,9,14,0,5,10,1,6,11,0,5,10,4,9,14);\} \end{aligned} \tag{21}$$

Such an FHS set is written as $\mathbb{C}(q, L, K, Z, H_m) = \mathbb{C}(15, 15, 5, 2, 3)$. The typical Hamming cross- and auto-correlations concerning the 1-st FHS ($C^{(1)}$) are shown in Tab. II. It is easy to verify that the Hamming correlations of the constructed FHS set meet the bounds in both (3) and (5) with equality. Thus, $\mathbb{C}$ in (21) is an *optimal* SNHZ-FHS set. For comparison, the Hamming correlations of an NHZ-FHS in [16] and a previous SNHZ-FHS set in [18] are also given in this table.

From Tab. II, it is found that when the shift-delay τ is limited within the zone Z (i.e., $|\tau| \le Z = 2$, as shown in Tab. II), the proposed SNHZ-FHS set enjoys orthogonality (i.e., $H_{uv} = H_{uu}(\tau \neq 0) = 0$). When $|\tau| > Z$, however, the maximum Hamming cross-correlation achieves a lower value ($H_{uv} = 3$) than that of the quasi-orthogonal NHZ-FHS constructed in [16] ($H_{uv} = 5$), at the cost of a slight increase of Hamming auto-correlation. In an FH multiple-access system, however, lowering the maximum Hamming cross-correlation is more important as it leads to a reduced amount of MAI. Noted that the Hamming correlation obtained in **Theorem 2** can also be verified by this example shown in Tab. II.

Overall, the Hamming correlation properties of the proposed SNHZ-FHS set are superior to the previous quasi-orthogonal NHZ-FH in [16] and traditional pseudo-random FHS in [12]. Again, it is noted that the proposed construction algorithm in

TABLE II
HAMMING CORRELATION VALUES OF THE SNHZ-FHS SET EXAMPLE IN (21) WITH Z=2.

$\tau_{1,v}$	-7	-6	-5	-4	-3	-2	-1	0	1	2	3	4	5	6	7
$H_{1,1}$	0	3	0	0	3	0	0	15	0	0	3	0	0	3	0
$H_{1,2}$	0	3	0	0	3	0	0	0	0	0	3	0	0	3	0
$H_{1,3}$	0	3	0	0	3	0	0	0	0	0	3	0	0	3	0
$H_{1,4}$	0	3	0	0	3	0	0	0	0	0	3	0	0	3	0
$H_{1,5}$	0	3	0	0	3	0	0	0	0	0	3	0	0	3	0
H_{uu} in [16]	0	0	0	0	0	0	0	15	0	0	0	0	0	0	0
H_{uv} in [16]	0	5	0	0	5	0	0	0	0	0	5	0	0	5	0
H_{uu} in [18]	0	3	0	0	3	0	0	15	0	0	3	0	0	3	0
H_{uv} in [18]	0	3	0	0	3	0	0	0	0	0	3	0	0	3	0
H_{uu} in [12]	0	0	0	0	0	0	0	15	0	0	0	0	0	0	0
H_{uv} in [12]	1	1	1	1	1	1	1	0	1	1	1	1	1	1	1

this paper is simpler than that in [18]. Whilst the proposed one is constructed via one optimal pseudo-random FHS set, the algorithm in [18] needs multiple specific pseudo-random FHS sets.

IV. TRANSCEIVER MODEL OF SNHZ-FH SYSTEM WITH BF TECHNIQUE

We consider a wireless network with multiple clusters as shown in Fig. 1, where the k-th user in a cluster is pre-assigned with the k-th SNHZ-FHS pattern $C^{(k)} = \left(c_0^{(k)}, c_1^{(k)}, \cdots, c_n^{(k)}, \cdots, c_{L-1}^{(k)}\right)$, in the SNHZ-FHS set $\mathbb{C}$ and $c_n^{(k)}$ is chosen from a given frequency-slot set with size q. Each cluster can support at most K active users by employing the proposed SNHZ-FHS set. Let us assume further that such a network is partitioned into K_c clusters according to the geographic locations and QoS requirements of users, in which one SNHZ-FHS set may be reused by these clusters. In this way, such a wireless network can accommodate at most $K_u = KK_c$ users in total over q frequency-slots.

At the user side, an FH signal with M-ary FSK modulation is sent from the transmitter[4]. For simplicity, it is assumed that one MFSK symbol with the interval T is transmitted during a hop and the minimum FH frequency spacing is sufficient to avoid the ISI [29]. At the BS side, an SNHZ-FH/BF receiver, as depicted in Fig. 2, is designed, in which a uniform linear array (ULA) with N_a-elements is adopted. The received signal in each antenna is first processed by a dehopper to obtain the MFSK baseband signal. In the dehopper, the local hopping pattern is synchronized with that in the desired transmitter. After the dehopping, a beamformer based on LMS-DMI algorithm is applied to generate the beam-pattern. The traditional SNHZ-FH system employing a single antenna investigated in [18] is unable to provide the beam-pattern to mitigate the interference in the space dimension. In contrast, the proposed SNHZ-FH/BF system outperforms the traditional one due to the combination of SNHZ-FH and multi-element array BF.

For multi-cluster uplink networks, we consider asynchronous transmissions where access delays $\{\tau^{(i,k)}\}_{i,k}$ of the k-th user in the i-th cluster are relaxed over arbitrary hopping intervals. Then, the transmitted signal of the i-th cluster during the n-th symbol interval can be written as

$$S^{(i)}(t)=\sum_{k=1}^{K}\sqrt{2P_k}\exp\left[j\left(2\pi\left(c_n^{(k)}\frac{M}{T}+\frac{d_n^{(i,k)}}{T}\right)(t-\tau^{(i,k)})+\phi_n^{(i,k)}\right)\right], \quad nT\le t\le (n+1)T, \tag{22}$$

where P_k denotes the transmit signal power of the k-th user. $d_n^{(i,k)} \in \{0, 1, \cdots, M-1\}$ denotes the current M-ary symbol, and $\phi_n^{(i,k)}$ stands for the random phase in the n-th MFSK symbol which is assumed to be an independent and identical uniform-distribution over $[-\pi, \pi)$.

Throughout this paper, we make the following assumptions concerning the network infrastructure: there is a large number of scatters distributed around users and there is a long distance between cluster and BS. Such a system setting is applicable to open space wireless propagation channels [5, 30]. Following these assumptions, the signal waveforms arrive at the array elements of BS through multiple independent propagation paths. Due to the multi-path propagation, the BF based on the direction-of-arrival (DoA) may suffer from performance loss. However, based on the channel knowledge at the transceiver, the BF weights may be optimized to match the channel

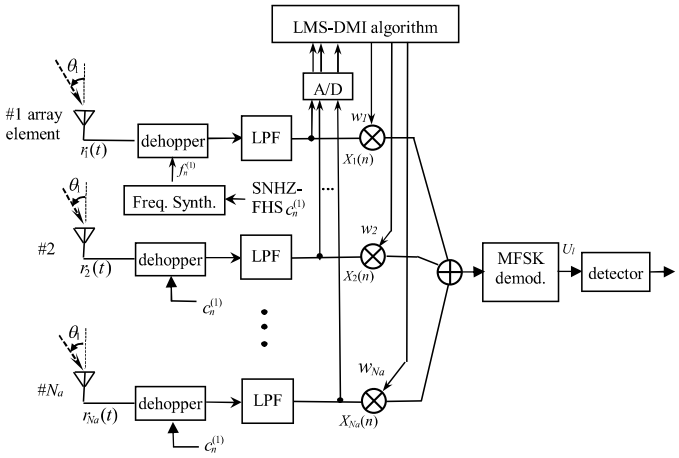

Fig. 2. The receiver model of the proposed SNHZ-FH/BF system (the 1-st cluster).

[4]Other modulation schemes, e.g., linear modulation, orthogonal frequency division multiplexing, may also be applied in the proposed system. For comparison with existing works (e.g., [9, 18, 25]), we only consider M-ary FSK modulation in this work.

characteristics for a desired user-cluster. The flat Rayleigh fading channel model is considered in this paper. As a result, the amplitude envelope $\sqrt{2P_k}$ undergoing the fading channel follows the Rayleigh distribution.

Furthermore, it is reasonable to assume that the width of main- and null-lobes can cover the areas of the desired and the interfering cluster with single DoAs respectively due to the small-scale clusters. That is, in this paper, the DoAs of all users in the cluster are simplified to a single DoA without the consideration of the distributions of users. The DoA of the center of the i-th cluster θ_i is randomly distributed over $[-\pi/2, \pi/2)$, where the angle θ_i is measured clock-wise from the boresight of the antenna array, as shown in Fig. 2. For a ULA with the inter-element spacing of $\delta_\Delta = cT/(2M)$ where c denotes the speed of light, the array steering-vector $\mathbf{a}_n^{(i)}$ corresponding to the n-th FH signal shown in (23), can be given by

$$\mathbf{a}_n^{(i)} = [1, \exp(j\Theta_i), \exp(j2\Theta_i), \cdots, \exp(j(N_a-1)\Theta_i)]^{\mathrm{T}}, \tag{23}$$

where $\Theta_i = 2\pi \sin(\theta_i)\delta_\Delta/\lambda_n$ and λ_n denotes the wavelength of the corresponding FH signal.

At the receiver of the BS, the total received signals from K_c clusters can be written as

$$\mathbf{r}(t) = \mathbf{A}_n \mathbf{S}(t) + \mathbf{n}(t), \tag{24}$$

where

$$\begin{aligned}
\mathbf{r}(t) &= [r_0(t), r_1(t), \cdots, r_{N_a-1}(t)]^{\mathrm{T}}, \\
\mathbf{S}(t) &= \left[S^{(1)}(t), S^{(2)}(t), \cdots, S^{(K_c)}(t)\right]^{\mathrm{T}}, \\
\mathbf{A}_n &= \left[\mathbf{a}_n^{(1)}, \mathbf{a}_n^{(2)}, \cdots, \mathbf{a}_n^{(K_c)}\right].
\end{aligned}$$

The noise vector is $\mathbf{n}(t) = [n_0(t), n_1(t), \cdots, n_{N_a-1}(t)]^{\mathrm{T}}$, in which each element is a zero-mean complex-valued white Gaussian noise with a two-sided power spectral density of $N_0/2$.

V. Signal Analysis for Interference Mitigation

In this section, we analyze the signals of the SNHZ-FH/BF system to explain the behavior of SNHZ-FH pattern and BF technique on the performance improvement in multi-cluster uplink networks. Then we derive the theoretical output signal-to-interference-plus-noise ratio (SINR) of the proposed system in order to evaluate the performance in terms of the convergence rate of the adaptive SNHZ-FH/BF receiver.

A. Interference Mitigation by SNHZ-FH Pattern

Without any loss of generality, we assume that 1) the 1-st user in the 1-st cluster is the desired user and 2) the desired transceiver has perfectly synchronised with the corresponding SNHZ-FH pattern, i.e., $\tau^{(1,1)} = 0$. The dehopped signal of the desired user is obtained as

$$\mathbf{X}(t) = \mathbf{r}(t)C(t), \tag{25}$$

where $C(t) = \exp(-j2\pi t c_n^{(1)} M/T)$ represents the local FH carrier driven by the local oscillator according to the pre-assigned SNHZ-FH pattern of the desired user (i.e., $k = 1$). The signal $\mathbf{X}(t)$ is processed through the low-pass-filter (LPF) with the bandwith $B_f = M/T$. Consequently, we obtain

$$\begin{aligned}
\mathbf{X}_f(t) = \hat{\mathbf{a}}_n^{(1)} \underbrace{\sqrt{2P_1}\exp\left(j2\pi \frac{d_n^{(1,1)}}{T} t + \phi_n^{(1,1)}\right)}_{\triangleq D(t)} + \underbrace{\sum_{k=2}^{K} I^{(1,k)}(t)}_{\triangleq I_{\text{intra}}(t)} \\
+ \sum_{i=2}^{K_c}\sum_{k=1}^{K} I^{(i,k)}(t) + \mathbf{n}(t), \quad nT \le t \le (n+1)T,
\end{aligned} \tag{26}$$

where $I^{(i,k)}(t)$ denotes the interference resulting from the k-th user in the i-th cluster. $\hat{\mathbf{a}}_n^{(i)}$ denotes the steering-vector imposed by the the MFSK symbol from the i-th cluster. The steering-vector $\hat{\mathbf{a}}_n^{(i)}$ can be rewritten as

$$\hat{\mathbf{a}}_n^{(i)} = \left[1, \exp(j\hat{\Theta}_i), \exp(j2\hat{\Theta}_i), \cdots, \exp(j(N_a-1)\hat{\Theta}_i)\right]^{\mathrm{T}}, \tag{27}$$

where $\hat{\Theta}_i = \pi \sin(\theta_i) d_n^{(i,k)}/M$.

Due to the asynchronous access in multi-cluster networks considered in this paper, there exists a relative delay $\tau^{(i,k)}$ in the desired receiver between the intra- and inter-cluster users. Thus, the delay $\tau^{(i,k)}$ can be expressed as

$$\tau^{(i,k)} = \Delta^{(i,k)} T + \rho^{(i,k)} T, \tag{28}$$

where the integer delay $\Delta^{(i,k)} = \lfloor \frac{\tau^{(i,k)}}{T} \rfloor$, and the fractional delay $\rho^{(i,k)} = (\tau^{(i,k)} - \Delta^{(i,k)}T)/T$. The symbol of the desired user may be impaired by the two adjacent hopping intervals, as shown in Fig. 3. Thus, the interference $I^{(i,k)}(t)$ shown in (26) is contributed by the two sub-intervals as follows [9]:

$$\begin{aligned}
&I^{(i,k)}(t) = I_1^{(i,k)}(t) + I_2^{(i,k)}(t) = \\
&h\left(c_{\hat{n}}^{(k)}, c_n^{(1)}\right) \hat{\mathbf{a}}_{\hat{n}}^{(i)} \sqrt{2P_k} \exp\left(j2\pi \frac{d_{\hat{n}}^{(i,k)}}{T} t + \phi_{\hat{n}}^{(i,k)}\right) G_1(t) \\
&+ h\left(c_{\hat{n}+1}^{(k)}, c_n^{(1)}\right) \hat{\mathbf{a}}_{\hat{n}+1}^{(i)} \sqrt{2P_k} \exp\left(j2\pi \frac{d_{\hat{n}+1}^{(i,k)}}{T} t + \phi_{\hat{n}+1}^{(i,k)}\right) G_2(t),
\end{aligned} \tag{29}$$

where the factor $\hat{n} := \hat{n}^{(i,k)} = n + \Delta^{(i,k)}$ denotes the index of FH slot of the k-th user in the i-th cluster after operating the delay $\tau^{(i,k)}$. The gate functions $G_1(t) = g_{(1-\rho^{(i,k)})T}(t - nT)$ and $G_2(t) = g_{\rho^{(i,k)}T}(t - nT - T + \rho^{(i,k)}T)$ with the following rectangular function

$$g_\nu(\mathrm{at}) = \begin{cases} 1, & 0 \le t \le \nu \\ 0, & \text{otherwise} \end{cases}. \tag{30}$$

From Tab. II, it is found that $h\left(c_{\hat{n}}^{(k)}, c_n^{(1)}\right) \equiv 0$ when $|\tau^{(i,k)}| \le ZT$. On the other hand, there may exist a few

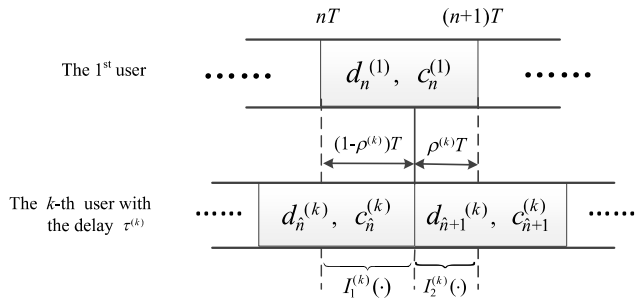

Fig. 3. The interference $I^{(i,k)}(t)$ contributing from the k-th user with the access delay of $\tau^{(i,k)}$, where the index i is omitted for simplicity.

frequency-hits (i.e., $h\left(c_{\hat{n}}^{(k)}, c_n^{(1)}\right) \neq 0$) when $|\tau^{(i,k)}| > ZT$. Thus, (26) can be rewritten as follows.

$$\mathbf{X}_f(t)=\begin{cases}\hat{\mathbf{a}}_n^{(1)} D(t) + \sum\limits_{i=2}^{K_c} I^{(i,1)}(t) + \mathbf{n}(t), & |\tau^{(i,k)}| \leq ZT, \\ \hat{\mathbf{a}}_n^{(1)} D(t) + I_{\text{intra}}(t) + \sum\limits_{i=2}^{K_c}\sum\limits_{k=1}^{K} I^{(i,k)}(t) + \mathbf{n}(t), & |\tau^{(i,k)}| > ZT. \end{cases} \tag{31}$$

Based on the above equation, the proposed SNHZ-FHS set offers orthogonality for $|\tau^{(i,k)}| \leq ZT$, i.e., intra-cluster interference-free. The amount of interference may increase when the same SNHZ-FH pattern are reused by other clusters for the large access delay $|\tau^{(i,k)}| > ZT$. However, it is noted that $I_{\text{intra}}(t)$ approaches to a minimum due to the quasi-orthogonality of the SNHZ-FH patterns [18].

In the following analysis, we focus on the asynchronous access scenario ($|\tau^{(i,k)}| > ZT$). The results for small access delay case ($|\tau^{(i,k)}| \leq ZT$) can be deduced from the former by setting $I_{\text{intra}}(t) = 0$ and $I^{(i,k)}(t) = 0, k \neq 1$, as illustrated in (31).

B. Interference Mitigation by Adaptive Array Antenna

In this subsection, we further utilize an adaptive BF technique to suppress the inter-cluster interference $I^{(i,k)}(t)$ as shown in (31). As a case study, an adaptive beamformer based on LMS-DMI algorithm is adopted in our proposed SNHZ-FH systems. Before the beamformer, the dehopped signal is sampled firstly, i.e.,

$$\mathbf{X}_N(n) = \mathbf{X}_f(nT_\Delta), \qquad n = 1, 2, \cdots, N, \tag{32}$$

where N denotes the number of samples for computing the weights of BF (i.e., the so-called snapshots), and T_Δ is the sample interval. It is assumed that $T_\Delta \ll \frac{1}{2f_{\max}}$, where $f_{\max}$ denotes the maximum frequency of FH signals. Suppose $D_p(n)$ is a pilot signal of the desired cluster, then the LMS-DMI algorithm is adopted to solve the following minimization problem [24]:

$$\min_{\mathbf{w}} |D_p(n) - \mathbf{w}^H \mathbf{X}_N(n)|^2. \tag{33}$$

The LMS-DMI algorithm can rapidly generate a stable beam-pattern by a short-length pilot signal. Then the optimal weights of array elements which are used in the beamformer can be computed by these N samples, i.e.,

$$\mathbf{w}_{DMI} = \mathbf{R}_{xx}^{-1}\mathbf{r}, \tag{34}$$

where

$$\begin{aligned} &\mathbf{R}_{xx} = \tfrac{1}{N}\mathbf{X}_N\mathbf{X}_N^H, \\ &\mathbf{r} = \tfrac{1}{N}\mathbf{d}^*\mathbf{X}_N, \\ &\mathbf{d} = [D_p(1), D_p(2), \cdots, D_p(N)]. \end{aligned} \tag{35}$$

Observed from (34) and (35), a larger N leads to more accurate $\mathbf{R}_{xx}$ and $\mathbf{r}$. However, this may increase the complexity of computation and implementation, resulting in a lower convergence rate.

The beam-pattern gain of the array antenna by the LMS-DMI BF algorithm can be shown as

$$g(\theta) = \mathbf{w}_{DMI}^H \hat{\mathbf{a}}_n^{(i)}(\theta). \tag{36}$$

Based on (31) and (34), the output signals of the LMS-DMI beamformer can be written as

$$\begin{aligned} y(t) &= \mathbf{w}_{DMI}^H \mathbf{X}_f(t) \\ &= \alpha^{(1)} D(t) + \alpha^{(1)} I_{\text{intra}}(t) + I_{\text{inter}}(t) + \mathbf{w}_{DMI}^H \mathbf{n}(t), \end{aligned} \tag{37}$$

where

$$\begin{aligned} \alpha^{(i)} &= \mathbf{w}_{DMI}^H \hat{\mathbf{a}}_n^{(i)}, \\ I_{\text{inter}}(t) &= \sum_{i=2}^{K_c} \alpha^{(i)} \sum_{k=1}^{K} I^{(i,k)}(t). \end{aligned}$$

Based on (37), the inter-cluster interference from the i-th cluster $I^{(i,k)}(t)$ can be further suppressed by multiplying the factor $\alpha^{(i)}$ of the proposed BF technique.

C. Output SINR and Beamforming Feature

Based on the samples of the signal (37), the output SINR of the proposed system can be written as

$$SINR = \frac{1}{N}\sum_{n=1}^{N} \frac{\left|\alpha^{(1)} D(n)\right|^2}{\left|\alpha^{(1)} I_{\text{intra}}(n) + I_{\text{inter}}(n)\right|^2 + \left|\mathbf{w}_{DMI}^H \mathbf{n}(n)\right|^2}. \tag{38}$$

In the receiver shown in Fig. 2, the non-coherent MFSK demodulator with M sub-branches is adopted, of which structure is elaborated in [29]. The decision variable U_l at the l-th sub-branch in the MFSK demodulator is shown as

$$U_l = \left| \int_0^T y(t) \exp\left(-j\frac{2\pi l t}{T}\right) dt \right|, \quad l = 0, 1, \cdots, M-1. \tag{39}$$

The detector chooses the index l corresponding to the largest U_l as the estimate of the desired user's symbol.

The convergence rate of the adaptive SNHZ-FH/BF receiver is studied in Fig. 4 by measuring the output SINR versus the number of snapshots (N). The key parameters of system include $SNR = 20$ dB and $N_a = 8$. From this figure, it is found that as N increases, the output SINR approaches to a stable value of 20 dB, indicating that the adaptive beamforming is effective in attaining convergence. The convergence rate of the proposed system is dependent on K_c and independent of the

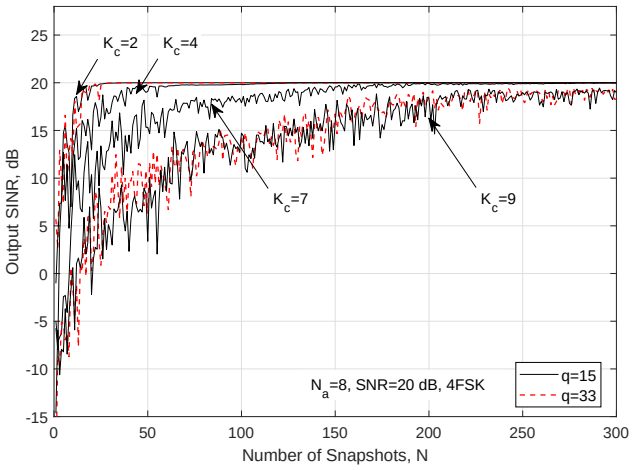

Fig. 4. The convergence rate of the adaptive SNHZ-FH/BF receiver under different numbers of snapshots (N).

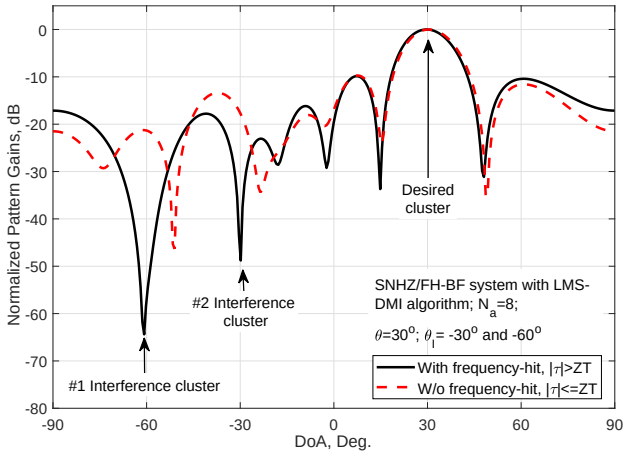

Fig. 5. The antenna beam-pattern gains of the proposed SNHZ-FH/BF system with N_a=8.

size of frequency-slot set ($q = 15$ and 30). For small K_c, we can see that the adaptive BF receiver is able to rapidly track the angular change of clusters over a small number of snapshots in the scenario of low mobility users/clusters. Thus, in the following analysis, it is reasonable to 1) assume that the convergence has been achieved during the short samples and 2) omit the effect of angular changes of clusters on the receive performance.

The normalized beam-pattern gains of the proposed SNHZ-FH/BF system with $N_a = 8$ array-elements generated by using $N = 200$ snapshots are shown in Fig. 5. We assume that the centric DoA from the desired cluster is $\theta_1 = 30°$ and those of the two interfering clusters $\theta_{\{I_1,I_2\}} = \{-30°, -60°\}$. Due to the networks setting with the small-scale cluster far away from the BS, the single DoA approximates the direction of the geographical center of cluster.

In Fig. 5, for the case of $|\tau^{(i,k)}| \leq ZT$, it is observed that the main lobe is directed towards the area of desired cluster ; however, since the interference has been already mitigated by the SNHZ-FH technique, the notches of null-lobes are not accurately formed at the directions of the interfering clusters.

For the case of $|\tau^{(i,k)}| > ZT$, the main- and null-lobes can be configured to direct towards the desired cluster and the interfering ones, respectively. In the following analysis, we assume that the vicinity of a single DoA of a null-lobe is wide enough to accommodate all the collocated users of an interfering cluster[5], and the beam pattern gains of the main-lobes and null-lobes are assumed to be constant over the areas of the desired and the interfering clusters.

VI. Performance Analysis

In this section, the theoretical error-rate performance of the proposed system is analyzed. Again, we assume that the desired user ($k = 1$) in the 1-st cluster transmits the symbol $d_n^{(1,1)} = 0$ during the n-th symbol interval.

By substituting (37) into (39), the decision variable U_l can be simplified as follows after a straightforward manipulation.

$$U_l = \left|\alpha^{(1)}\sqrt{2P_1}\delta_{0,l} + \alpha^{(1)} I'_{\text{intra}} + I'_{\text{inter}} + n'\right|, \quad l = 0, 1, \cdots, M-1, \tag{40}$$

where $\delta_{0,l} = 1$ for $l = 0$ and 0 otherwise, n' denotes a Gaussian random variable with zero mean and variance $N_0/2$, and

$$I'_{\text{intra}} = \sum_{k=2}^{K} \underbrace{\int_0^T I^{(1,k)}(t) \exp\left(-j\frac{2\pi lt}{T}\right) dt}_{\triangleq I'^{(1,k)}}, \tag{41}$$

$$I'_{\text{inter}} = \sum_{i=2}^{K_c} \alpha^{(i)} \sum_{k=1}^{K} \underbrace{\int_0^T I^{(i,k)}(t) \exp\left(-j\frac{2\pi lt}{T}\right) dt}_{\triangleq I'^{(i,k)}}. \tag{42}$$

Then, the summation of intra- and inter-cluster interferences in (40) can be obtained as

$$\alpha^{(1)} I'_{\text{intra}} + I'_{\text{inter}} = \sum_{i=1}^{K_c}\sum_{k=1}^{K} \alpha^{(i)} I'^{(i,k)} - \alpha^{(1)} I'^{(1,1)}, \tag{43}$$

where $I'^{(i,1)}$ denotes the self-interference of the user in the i-th cluster imposed by the reuse of the desired user's SNHZ-FH pattern. For the case of $i \neq 1$, $I'^{(i,1)}$ is determined by the Hamming out-of-phase auto-correlation of such an SNHZ-FH pattern[6]. From **Theorem 2** (as illustrated in Tab. II), it is observed that the Hamming out-of-phase auto-correlation is equivalent to Hamming cross-correlation, which helps to simplify the subsequent derivations.

[5]In practice, as pointed by one reviewer, it is also likely that the interfering users are arbitrarily distributed. Throughout this work, however, it is assumed a proper user grouping algorithm has been carried out such that the collocated users are grouped into one cluster.

[6]Actually, due to the different geographic locations of multiple clusters, those users that reuse the same SNHZ-FH pattern in other clusters may not be fully synchronized with the desired one. Therefore, the Hamming out-of-phase auto-correlations of the SNHZ-FH pattern is the dominant factor impacting $I'^{(i,1)}$.

Substituting (29) into $I'^{(i,k)}$, the interference $I'^{(i,k)}$ can be rewritten as

$$I'^{(i,k)} = h\left(c_{\hat{n}}^{(k)}, c_n^{(1)}\right)\int_0^{(1-\rho^{(i,k)})T}\sqrt{2P_k}\exp\left(j2\pi\frac{d_{\hat{n}}^{(i,k)}-l}{T}t\right)dt + h\left(c_{\hat{n}+1}^{(k)}, c_n^{(1)}\right)\int_{(1-\rho^{(i,k)})T}^{T}\sqrt{2P_k}\exp\left(j2\pi\frac{d_{\hat{n}+1}^{(i,k)}-l}{T}t\right)dt. \quad (44)$$

For ease of analysis, it is also assumed that perfect power control is carried out with the aid of pilot signals. Hence, no consideration is given to the geographic distributions of clusters (and users) as well as the resultant path-losses between BS and users. Moreover, the received signal power for each user in multi-cluster networks follows an independent and identical Rayleigh distribution. Thus, the average energy per received symbol is $\overline{E_s} = \overline{E_k} = \overline{P_k}T$ for all k's, where $\overline{P_k}$ denotes the average power at the receiver side.

Given the pre-assigned SNHZ-FHS set $\mathbb{C}$ and the access delay $\{\tau^{(i,k)}\}_{i,k}$, the conditional probability-density-function (pdf) of the decision variable U_l over the Rayleigh fading channel can be expressed as [29],

$$p_{U_l|\mathbb{C},\tau}(u_l) = \frac{u_l}{\sigma_l^2}\exp\left(-\frac{u_l^2}{2\sigma_l^2}\right), \quad (45)$$

where

$$\begin{aligned}\sigma_l^2 =& \frac{1}{2}\Big(\delta_{0,l}(\alpha^{(1)})^2\overline{E_s} \\ &+ \sum_{i=1}^{K_c}\sum_{k=1}^{K} h\left(c_{\hat{n}}^{(k)}, c_n^{(1)}\right)(1-\rho^{(i,k)})(\alpha^{(i)})^2\delta_{l,d_{\hat{n}}^{(i,k)}}\overline{E_s} \\ &+ \sum_{i=1}^{K_c}\sum_{k=1}^{K} h\left(c_{\hat{n}+1}^{(k)}, c_n^{(1)}\right)\rho^{(i,k)}(\alpha^{(i)})^2\delta_{l,d_{\hat{n}+1}^{(i,k)}}\overline{E_s} \\ &+ h\left(c_{\hat{n}}^{(1)}, c_n^{(1)}\right)(1-\rho^{(1,1)})(\alpha^{(1)})^2\delta_{l,d_{\hat{n}}^{(1,1)}}\overline{E_s} \\ &+ h\left(c_{\hat{n}+1}^{(1)}, c_n^{(1)}\right)\rho^{(1,1)}(\alpha^{(1)})^2\delta_{l,d_{\hat{n}+1}^{(1,1)}}\overline{E_s} + N_0\Big). \quad (46)\end{aligned}$$

After the no-coherent MFSK demodulation, the conditional symbol-error-rate (SER) of the proposed SNHZ-FH/BF system is computed as

$$\begin{aligned}P_{e|\mathbb{C},\tau} &= 1 - \int_0^{\infty} P(U_l < U_0, l = 1, 2, \cdots, M-1)p_{U_0|\mathbb{C},\tau}(u_0)du_0 \\ &= 1 - \int_0^{\infty} p_{U_0|\mathbb{C},\tau}(u_0)\left[\int_0^{u_0} p_{U_l|\mathbb{C},\tau}(u_l)du_l\right]^{M-1}du_0 \\ &= 1 - \int_0^{\infty} p_{U_0|\mathbb{C},\tau}(u_0)\left[1-\exp\left(-\frac{u_0^2}{\sigma_l^2}\right)\right]^{M-1}du_0, \quad (47)\end{aligned}$$

where $P(U_l < U_0, l = 1, 2, \cdots, M-1)$ denotes the joint probability that $\{U_l\}_l$ are all less than U_0.

For a given maximum access delay τ_M, we assert that the integer delay $\Delta^{(i,k)}$ and the fractional delay $\rho^{(i,k)}$ follow the uniform-distributions over $\{-\lfloor\tau_M/T\rfloor, -\lfloor\tau_M/T\rfloor + 1, \cdots, \lfloor\tau_M/T\rfloor - 1, \lfloor\tau_M/T\rfloor\}$ and $[0, 1)$ for all k's and i's, respectively. Then, the average SER can be computed as follows by evaluating the expectation over the delay $\tau^{(i,k)}$.

$$\overline{P}_{e|\mathbb{C}} = \mathbb{E}_\tau\{P_{e|\mathbb{C},\tau}\} = \frac{1}{2\lfloor\frac{\tau_M}{T}\rfloor+1}\sum_{\Delta=-\lfloor\frac{\tau_M}{T}\rfloor}^{\lfloor\frac{\tau_M}{T}\rfloor}\int_0^1 P_{e|\mathbb{C},\tau}d\rho. \quad (48)$$

For the special case of $|\tau^{(i,k)}| \le \tau_M \le ZT$, we have $h\left(c_{\hat{n}}^{(k)}, c_n^{(1)}\right) = h\left(c_{\hat{n}+1}^{(k)}, c_n^{(1)}\right) \equiv 0$ for all k's (including the Hamming out-of-phase auto-correlation). Then the SER can also be computed by (48) with the specific parameter σ_l^2 by setting $K = 1$ in (46).

The average BER of the proposed SNHZ-FH/BF system can be computed as

$$\overline{P}_{b|\mathbb{C}} = \frac{2^{\log_2(M)-1}}{M-1}\overline{P}_{e|\mathbb{C}}. \quad (49)$$

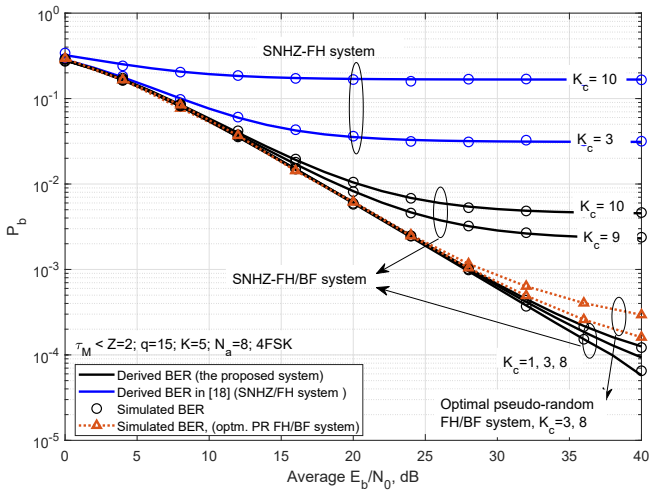

Fig. 6. Average BER comparisons among the proposed SNHZ-FH/BF, the optimal pseudo-random FH/BF and traditional SNHZ-FH under 4FSK modulation.

VII. Numerical Comparisons

In this section, we investigate the BER performances of SNHZ-FHS/BF system through numerical comparisons. We recall the following assumptions for the networks infrastructure and parameters setup: 1) K_c non-overlapping clusters, each of which accommodates K users at most, are served by a receiver deployed at the BS. 2) This receiver is equipped with a uniform linear array with N_a elements and half-wavelength spacing. 3) Perfect power control has been achieved among all users and the DoA angles of the clusters are uniformly and randomly distributed over $[-\pi/2, \pi/2)$ without consideration of the geographic distributions of users and clusters. Besides, for comparison, *traditional* SNHZ-FH system [18] and an *optimal pseudo-random* FH system with the array beamformer system (i.e., *optim. PR FH/BF*), are also evaluated. The adopted SNHZ-FH patterns are generated by the proposed construction as shown in Section III.

Average BER comparisons among the proposed SNHZ-FH/BF system, the optimal pseudo-random FH/BF system and

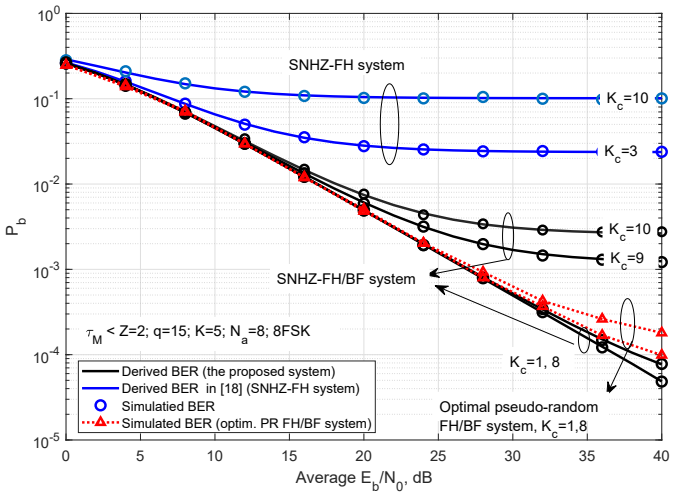

Fig. 7. Average BER comparisons among the proposed SNHZ-FH/BF, the optimal pseudo-random FH/BF and traditional SNHZ-FH under 8FSK modulation.

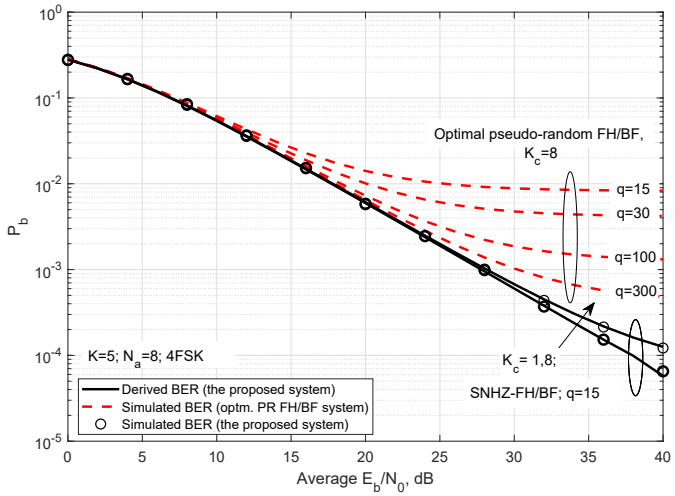

Fig. 8. Average BER comparisons of the proposed SNHZ-FH/BF with optimal pseudo-random FH/BF under 4FSK modulation.

traditional SNHZ-FH for the access delays $|\tau^{(i,k)}| \leq ZT$ are shown in Fig. 6 for 4FSK and in Fig. 7 for 8FSK. For a small amount of user-clusters, i.e., $K_c \leq 8$, the proposed SNHZ-FH/BF system can mitigate almost all the interference and hence the resulting BERs approach to those of the single-user ($K_c = 1$). For a large K_c, the BER performance of the proposed SNHZ-FH/BF system gets deteriorated, but still outperforms that of traditional SNHZ-FH. Besides, the proposed SNHZ-FH/BF exhibits superior BER performance compared to that of optimal pseudo-random FH/BF, thanks to the fact that the employed SNHZ-FH patterns lead to zero intra-cluster interference which may not be met by the latter. The BER behaviors of 8FSK modulation are omitted as they are similar to the case of 4FSK. One can also observe from these two figures that the derived BER curves calculated via (49) well match with the simulated BERs labeled by circle marker.

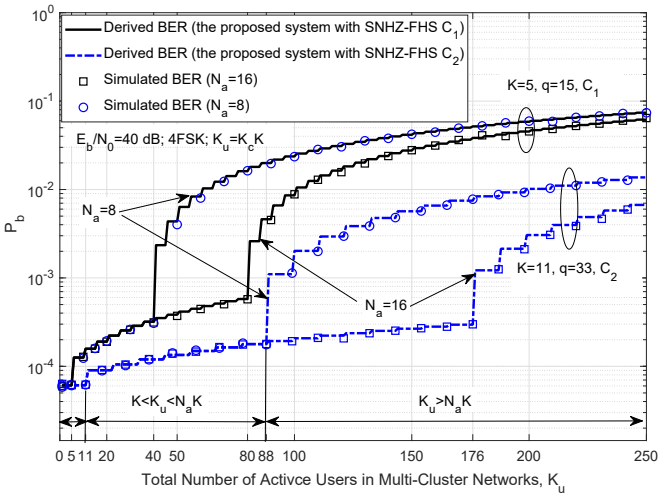

Fig. 9. Average BERs of the proposed SNHZ-FH/BF system versus the total number of active users over multi-cluster networks (K_u).

The error rate advantage of the proposed *optimal* SNHZ-FH/BF compared to *optimal pseudo-random* FH/BF is presented in Fig. 8. Based on the properties of optimal pseudo-random FH patterns [10–12], it can be readily shown that the probability of at least one collision over each frequency slot is approximated by $r_h = 1 - (1 - 1/q)^{K_c K - 1}$ for the entire multi-cluster network. Consequently, the BER performance of *optimal pseudo-random FH/BF* can only be improved by increasing q, as shown in Fig. 8. In comparison, the proposed SNHZ-FH/BF system with a small value of $q = 15$ still outperforms the optimal pseudo-random FH/BF with a large value of $q = 300$, thus leading to certain spectral gain under band-limited condition.

The BER performances of the proposed SNHZ-FH/BF system for different number of active users (K_u) in multi-cluster networks are plotted in Fig. 9. Two classes of SNHZ-FH patterns are applied, i.e., $\mathbb{C}(q, L, K, Z, H_m) = \mathbb{C}_1(15, 15, 5, 2, 3)$ and $\mathbb{C}_2(33, 33, 11, 2, 3)$. Besides, two types of ULAs with $N_a = 8$ and $N_a = 16$ are also considered.

First, let us consider the combination of $\mathbb{C}_2$ and $N_a = 8$ in Fig. 9 to explain the BER behaviors of the proposed SNHZ-FH/BF system. For $K_u \leq K = 11$, the BER is independent of the number of active users, thanks to the interference elimination property of the adopted SNHZ-FH patterns. For $K < K_u \leq N_a K = 88$, the BER suffers a slight increase. This is because the antenna array with $N_a = 8$ can provide at most $N_a - 1$ notches of beam-pattern (as shown in Fig. 5) to cover those interfering clusters. In this case, a significantly large portion of inter-cluster interference is mitigated by the proposed BF receiver. In the case of $K_u > KN_a = 88$, the integration of SNHZ-FHS and BF techniques is incapable of offering enough degrees of freedom in spectral and spatial domains to combat the interference, thus giving rise to gradual BER deterioration. From the above analysis, one can see that the proposed SNHZ-FH/BF structure is capable of accommodating more active users with an enhanced/acceptable BER performance. As expected, one can notice that large N_a and q lead to improved BER performances.

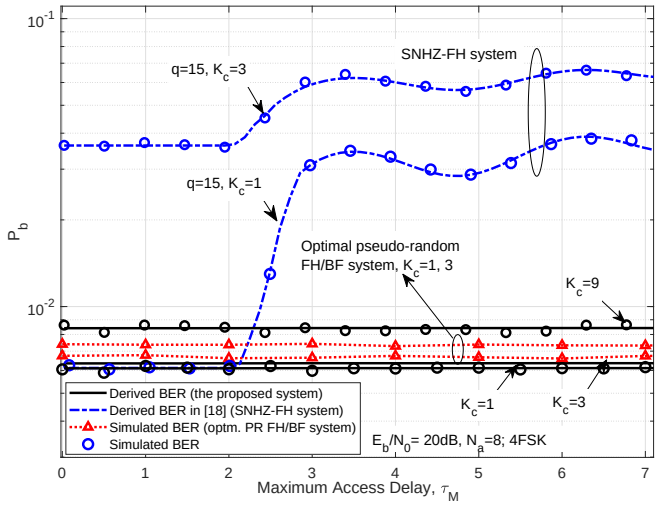

Fig. 10. Average BER comparisons of the proposed SNHZ-FH/BF system with the change of the maximum access delay τ_M.

In Fig. 9, it is also noted that the theoretical BER increases in a step size of K (i.e., the size of SNHZ-FHS set) as K_u grows. The reason lies in the fact that the residual inter-cluster interference after the BF interference elimination is only dependent on that specific reused FH pattern and the inter- and intra-cluster interferences from the other $K-1$ FH patterns (shared in multiple clusters) can be completely mitigated owing to the orthogonality property of the proposed SNHZ-FHS set.

The BERs of the proposed SNHZ-FH/BF system for various maximum access delays τ_M are presented in Fig. 10, where the access delay of each user $\{\tau^{(i,k)}\}$ is assumed to be i.i.d over $[-\tau_M, \tau_M]$ for all k's and i's. For comparison, the BERs of traditional SNHZ-FH are also plotted[7], where the BER performance heavily depends on specific Hamming correlation values corresponding to the time delay τ. In contrast, the BERs of the proposed SNHZ-FH/BF system are almost independent of the delay but dependent on K_c (i.e., depending on inter-cluster interference). Moreover, the proposed SNHZ-FH/BF system leads to an enhanced BER performance compared to both of the traditional SNHZ-FH and the optimal pseudo-random FH/BF under the same system settings. From the timing synchronization point of view, the proposed SNHZ-FH/BF system is capable of tolerating larger access delays as shown in Fig. 10.

In this section, although we only consider $q = 15, 33$ and 4FSK, 8FSK for verification of the theoretical results, our proposed SNHZ-FH/BF design algorithm is applicable to other values of q and/or FSK modulation orders.

VIII. Conclusions and Future Work

This paper is dedicated to the design and analysis of an enhanced FH system, aiming for the enabling of massive connectivity in multi-cluster uplink networks with limited spectrum resources. As an improvement of our earlier proposed SNHZ-FH technique in [18], we have first developed a refined construction of *optimal* SNHZ-FHS set based on one seed FHS set (in contrast, multiple seed FH sets are needed in [18]). We have derived the properties of the proposed SNHZ-FHS set, including its Hamming correlation values at different time-shifts, as shown in **Theorem 2**. Such an optimal SNHZ-FHS set enjoys orthogonality for access delays within the no-hit zone and quasi-orthogonality otherwise, compared to the traditional pseudo-random FHS sets.

To improve the user capacity for multi-cluster networks, we have integrated the developed SNHZ-FH with a novel array BF receiver called SNHZ-FH/BF. We have shown that the area of the user-cluster of interest can be adaptively covered by the main-lobes of BF, whilst rejecting the other inter-cluster users by taking advantage of the beam null-lobes. As a case study, we have studied the adaptive BF with the LMS-DMI algorithm of the proposed system. Moreover, we have investigated the impacts of the SNHZ-FHS parameters (e.g., q, K and H_m), the array's parameter (e.g., N_a) and the networks' parameters (e.g., K_u and K_c) on the BER performance through extensive theoretical and simulation results.

Compared to traditional SNHZ-FH in [18] and pseudo-random FH/BF, our proposed SNHZ-FH/BF system provides a promising means for multi-cluster networks due to its large multi-user capacity and enhanced BER performances. Furthermore, our proposed SNHZ-FH/BF is almost insensitive to the access delay, which is an important merit for asynchronous multi-cluster transmissions.

Future Works: In order to simplify the analysis, we have made several assumptions regarding the system infrastructure and parameter setups. For example, perfect power control is assumed throughput this paper. As we focus on the enabling of massive connectivity in 5G/B5G networks in which a huge number of communication devices are densely deployed over a small area, power control is relatively easy to carry out. For massive connectivity serving large-scale geographical areas, as pointed by one reviewer, power control may result in 1) a very large dynamic range for the user terminal transmit powers and 2) significant increase of inter-cell interference in a cellular environment. In this case, it would be interesting to understand how practical issues of power control can affect the system design from the FHS construction to enhanced receiver development.

In recent years, another important paradigm for massive connectivity is non-orthogonal multiple access (NOMA) where multiple users transmit over the same time-frequency resources [31–33]. Among many NOMA schemes, there are two major classes of NOMA systems where multiple users are separated in power- and code- domains, respectively. Future research may be conducted on integration of NOMA and FH systems. Instead of treating multiuser interference as a noise term, as in most FH literature, how to design a new receiver based on, for example, successive interference cancellation or message passing algorithm, is worthy of a deeper study. New FH patterns may also be designed for the envisaged NOMA-FH systems.

[7]A detailed study of BER behaviors of traditional SNHZ-FH with regard to τ_M can be found in [18].

IX. Acknowledgement

The authors are deeply indebted to the anonymous Reviewers for many of their insightful comments which have greatly helped improve the quality of this work.

References

[1] L. Dai, B. Wang, S. Han and *et al*., "Non-orthogonal multiple access for 5G: solutions, challenges, opportunities, and future research trends," *IEEE Commun. Mag.*, vol. 53, no. 9, pp. 74-81, Sep. 2015.

[2] K. J. Kim, P. L. Yeoh and *et al*., "A multi-cluster-based distributed CDD scheme for asynchronous joint transmissions in local and private wireless networks," *IEEE Trans. Wireless Commun.*, 2021, early access.

[3] Bluetooth Special Interest Group (SIG). (2016). Bluetooth Specification, 683 Version 5.0. [Online]. Available: http://www.bluetooth.org.

[4] Q. Zeng, H. Li, and D. Peng, "Frequency-hopping based communication network with multi-level QoS's in smart grid: code design and performance analysis," *IEEE Trans. Smart Grid*, vol. 3, no. 4, pp. 1841-1852, Dec. 2012.

[5] D. Torrieri, S. Talarico, and M. C. Valenti, "Analysis of a frequency-hopping millimeter-wave cellular uplink," *IEEE Trans. Wireless Commun.*, vol. 15, no. 10, pp. 7089-7098, Oct. 2016.

[6] P. Fan and M. Darnell, *Sequence Design for Communications Applications*, U.K.: Research Studies Press (RSP), 1996.

[7] M. Lin *et al*., "Frequency-hopping CDMA with Reed-Solomon code sequences in wireless communications," *IEEE Trans. Commun.*, vol. 55, no. 11, pp. 2052-2055, Nov. 2007.

[8] A. J. Al-Dweik and B. S. Sharif, "Exact performance analysis of synchronous FH-MFSK wireless networks," *IEEE Trans. Veh. Technol.*, vol. 58, no. 7, pp. 3771-3776, Sep. 2009.

[9] K. Choi and K. Cheun, "Performance of asynchronous slow frequency-hop multiple-access networks with MFSK modulation," *IEEE Trans. Commun.*, vol. 48, no. 2, pp. 298-307, Feb. 2000.

[10] L. Guan, Z. Li, J. Si, and B. Hao, "Analysis of asynchronous frequency hopping multiple-access network performance based on the frequency hopping sequences," *IET Commun.*, vol. 9, no.1, pp. 117-121, Jan. 2015.

[11] D. Y. Peng and P. Z. Fan, "Lower bounds on the Hamming auto-and cross-correlations of frequency-hopping sequences," *IEEE Trans. Inf. Theory*, vol. 50, no. 9, pp. 2149-2153, Sep. 2004.

[12] Z. Zhou, X. Tang, D. Peng, and U. Parampalli, "New constructions for optimal sets of frequency-hopping sequences," *IEEE Trans. Inf. Theory*, vol. 57, no. 6, pp. 3831-3840, Jun. 2011.

[13] C. Ding, R. Fuji-Hara, Y. Fujiwara and *et al*., "Sets of frequency hopping sequences: bounds and optimal constructions," *IEEE Trans Inf. Theory*, vol. 55, no. 7, pp. 3297-3304, July 2019.

[14] J. H. Chung, G. Gong, and K. Yang, "New families of optimal frequency-hopping sequences of composite lengths," *IEEE Trans. Inf. Theory*, vol. 60, no. 6, pp. 3688-3697, Apr. 2014.

[15] X. Liu, L. Zhou, and Q. Zeng, "No-hit-zone frequency hopping sequence sets with respect to aperiodic Hamming correlation," *Electron. Lett.*, vol. 54, no. 4, pp. 212-213, Feb. 2018.

[16] W. X. Ye, P. Z. Fan, and E. M. Gabidulin, "Construction of non-repeating frequency-hopping sequences with no-hit zone," *Electron. Lett.*, vol. 42, no. 12, pp. 681-682, Jun. 2006.

[17] Q. Zeng and X. Liu, "Chaos theory-based NHZ-FH sequence set for quasi-synchronous FHMA system," *Electron. Lett.*, vol. 53, no. 22, pp. 1493-1495, Sep. 2017.

[18] Q. Zeng, Z. Z. Zhou, X. Liu, and Z. L. Liu, "Strong no-hit-zone sequences for improved quasi-orthogonal FHMA systems: sequence design and performance analysis," *IEEE Trans. Commun.*, vol. 67, no. 8, pp. 5336-5345, Aug. 2019.

[19] W. X. Ye, P. Z. Fan and *et al*., "Theoretical bound on no hit zone of frequency hopping sequences," in *Proc. 5th Int. Workshop in Signal Design Its Appl. Commun.*, Guilin, China, pp. 115-117, Oct. 2011.

[20] Z. Liu, U. Parampalli, and Y. L. Guan, "Optimal odd-length binary Z-complementary pairs," *IEEE Trans. Inf. Theory*, vol. 60, no. 9, pp. 5768-5781, Sep. 2014.

[21] Z. C. Zhou, D. Zhang, T. Helleseth, and J. Wen, "A construction of multiple optimal ZCZ sequence sets with good cross correlation," *IEEE Inf. Theory*, vol. 64, no. 2, pp. 1340-1346, Feb. 2018.

[22] S. Chen, S. Sun, Q. Gao, and X. Su, "Adaptive beamforming in TDD-based mobile communication systems: State of the art and 5G research directions," *IEEE Wireless Commun.*, vol. 23, no. 6, pp. 81-87, Dec. 2016.

[23] Z. Zhang, K. C. Teh, and K. H. Li, "Performance analysis of two-dimensional massive antenna arrays for future mobile networks," *IEEE Trans. Veh. Technol.*, vol. 64, no. 11, pp. 5400-5405, Nov. 2015.

[24] A. Sharma and S. Mathur, "Performance analysis of adaptive array signal processing algorithms," *IETE Tech. Rev.*, vol. 33, no. 5, pp. 472-491, May 2016.

[25] Q. Zeng, X. Liu, and J. Zhong, "An improved frequency-hopping system with no-hit-zone hopping pattern based on adaptive array receiver for anti-interference," in *Proc. IEEE Veh. Technol. Conf.*, Kuala Lumpur, Malaysia, Apr. 28-May. 2, 2019.

[26] K. T. Wong, "Acoustic vector-sensor FFH "blind" beamforming & geolocation," *IEEE Trans. Aerospace and Electron. Systs.*, vol. 46, no. 1, pp. 444-449, Jan. 2010.

[27] Q. Zeng, H. Nasser, and G. Gradoni, "A secure waveform format for interference mitigation in heterogeneous uplink networks," *IEEE Access*, vol. 6, pp. 41688-41696, Aug. 2018.

[28] Y.-P. E. Wang, X. Lin, A. Adhikary, A. Grovlen, Y. Sui, Y. Blankenship, J. Bergman, and H. S. Razaghi, "A primer on 3GPP narrowband internet of things," *IEEE Commun. Mag.*, vol. 55, no. 3, pp. 117-123, Mar. 2017.

[29] J. G. Proakis and M. Salehi, *Digital Communications* (5th edition). New York, USA: McGraw-Hill, 2007.

[30] S. Chen, S. Sun, Q. Gao, and X. Su, "Adaptive beamforming in TDD-based mobile communication systems: state of the art and 5G research directions," *IEEE Wireless Commun.*, vol. 23, no. 6, pp. 81-87, Dec. 2016.

[31] Y. Liu, Z. Qin, M. Elkashlan, Z. Ding, A. Nallanathan, and L. Hanzo, "Nonorthogonal multiple access for 5G and beyond," *Proceedings of the IEEE*, vol. 105, no. 12, pp. 2347-2381, Dec. 2017.

[32] F. Wei, W. Chen, Y. Wu, and *et al*., "Toward 5G wireless interface technology: enabling nonorthogonal multiple access in the sparse code domain," *IEEE Vehi. Tech. Mag.*, vol. 13, no. 4, pp. 18-27, Dec. 2018.

[33] Z. Liu and L.-L. Yang, "Sparse or dense: a comparative study of code-domain NOMA systems," *IEEE Trans. Wireless Commun.*, vol. 20, no. 8, pp. 4768-4780, Aug. 2021.